

A superconducting bolometer with strong electrothermal feedback

Adrian T. Lee^{a)} and Paul L. Richards^{b)}

Department of Physics, University of California, Berkeley, California 94720

Sae Woo Nam and Blas Cabrera

Department of Physics, Stanford University, Stanford, California 94305-4060

K. D. Irwin

National Institute of Science and Technology, Boulder, Colorado 80303

(Received 15 May 1996; accepted for publication 5 July 1996)

We present a theoretical analysis and experimental evaluation of a transition-edge superconducting bolometer for detecting infrared and millimeter waves. The superconducting film is voltage biased and the current is read by a superconducting quantum interference device ammeter. Strong electrothermal feedback maintains the sensor temperature within the transition, gives a current responsivity that is simply the inverse of the bias voltage, and reduces the response time by several orders of magnitude below the intrinsic time constant C/G . We evaluated a voltage-biased bolometer that operates on the $T_c \sim 95$ mK transition of a tungsten film with a thermal conductance of $G \sim 1.2 \times 10^{-9}$ W/K. As expected, the electrical noise equivalent power of 3.3×10^{-17} W/ $\sqrt{\text{Hz}}$ is close to the thermal fluctuation noise limit and is lower than that of other technologies for these values of G and temperature. The measured time constant of $10 \mu\text{s}$ is ~ 100 times faster than the intrinsic time constant. © 1996 American Institute of Physics. [S0003-6951(96)00136-2]

Cryogenic bolometers are sensitive detectors of infrared and millimeter wave radiation and are widely used in laboratory experiments as well as ground-based, airborne, and space-based astronomical observations.¹ In many applications, bolometer performance is limited by a trade off between speed and sensitivity. In this letter, we describe a novel superconducting transition-edge bolometer that can give a large increase in speed and a significant increase in sensitivity over technologies now in use. This combination of speed with sensitivity should open new applications for bolometric detectors.

Current-biased superconducting bolometers² have long been studied, but not widely used, due to a lack of a compelling performance advantage and complexities in their operation. Recently, Irwin^{3,4} has described a particle detector based on a voltage-biased superconducting film that maintains itself in the transition region through the use of strong negative electrothermal feedback (ETF). This detector was superior to current-biased particle detectors in terms of linearity, resolution, and maximum count rate. We consider the benefits of this mode of operation for bolometric detection⁵ of infrared and millimeter waves. We call this device a voltage-biased superconducting bolometer (VSB).

Electrothermal feedback arises from the dependence of the bias power on the resistance of the superconductor. If there is an increase in optical power incident on the bolometer, the temperature rises, the resistance increases and, for constant voltage bias, the sensor current decreases. If the transition is steep enough, the resulting decrease in bias power nearly compensates for the increase in incident power and the temperature of the device remains essentially constant. The strength of the feedback is proportional to $\alpha =$

$d \log R/d \log T$, which can exceed 10^3 for superconducting films. The change in bias current is read out with a superconducting quantum interference device (SQUID) ammeter. There are several important benefits to this mode of operation aside from the stable self-bias: (i) Since the temperature is held nearly constant, the thermal response time is greatly reduced. The thermal time constant is inversely proportional to α . (ii) The noise equivalent power (NEP) can be at the thermal fluctuation limit, due to the low noise of SQUID ammeters and negligible Johnson noise.^{3,6} (iii) The responsivity of the detector is given by the inverse of the bias voltage, regardless of optical load, which greatly simplifies calibration for quantitative measurements.

The responsivity of the VSB can be derived from an equation describing the power flow,

$$P + \delta P e^{i\omega t} + V_b^2/R - (V_b^2\alpha/RT) \delta T e^{i\omega t} = \bar{G}(T - T_0) + G \delta T e^{i\omega t} + i\omega C \delta T e^{i\omega t}. \quad (1)$$

Here, P is the constant optical background power on the bolometer, $\delta P \ll P$ is the signal power at angular frequency ω , V_b is the voltage bias, R is the steady-state resistance, and T and $\delta T \ll T$ represent the steady-state and time-varying temperatures of the sensor. Power flow to the heat sink at temperature T_0 is governed by the differential and average thermal conductances $G = \delta P/\delta T$ and $\bar{G} = (P + P_b)/(T - T_0)$, where $P_b = V_b^2/R$. Energy is also stored in the heat capacity C of the bolometer. The fourth term of Eq. (1) gives the ETF. The current responsivity S_I is given by

$$S_I \equiv \frac{\delta I}{\delta P} = -\frac{V_b\alpha}{RT} \left(G + i\omega C + \frac{V_b^2\alpha}{RT} \right)^{-1} \sim -\frac{1}{V_b} \left(\frac{1}{1 + i\omega\tau} \right), \quad (2)$$

where δI is the time varying sensor current. The approximation is valid for $V_b\alpha/(RTG) \gg 1$, which is easily achieved for large α . This ratio describes the strength of the feedback. The response time τ can be written as

^{a)}Also at Center for Particle Astrophysics, University of California, Berkeley, California 94720. Electronic mail: atl@physics.berkeley.edu

^{b)}Materials Science Division, Lawrence Berkeley National Laboratory, University of California, Berkeley, California 94720.

$$\tau = \frac{C}{G} \left(1 + \frac{V_b^2 \alpha}{RTG} \right)^{-1} = \frac{C}{G} \left[1 + \frac{\bar{G}}{G} \left(1 - \frac{T_0}{T} \right) \alpha F_b \right]^{-1} \sim \frac{C}{G} \frac{n}{\alpha F_b}, \quad (3)$$

where $F_b = P_b / (P + P_b)$ and the power flow is assumed to be given by $(P + P_b) \propto T^n - T_0^n$, so $G \propto T^{n-1}$. We have used the exact expression, $G/\bar{G} = n(1 - T_0/T) / [1 - T^n \gg T_0^n]$, in the $T^n \gg T_0^n$ limit to obtain the approximation in Eq. (3).

The NEP for $\omega \ll 1/\tau$ can be written⁶

$$\text{NEP}^2 = \gamma 4kT^2 G + \frac{1}{S_I^2} \left[i_n^2 + \left(\frac{\tau}{\tau_0} \right)^2 \left(\frac{4kT}{R} + A(\omega) \right) \right], \quad (4)$$

where the terms describe thermal fluctuation noise, SQUID noise, Johnson noise, and intrinsic 1/f fluctuations in the superconductor, respectively. The parameter γ describes the reduction in phonon noise from the thermal equilibrium value due to the difference in temperature between the sensor and the sink.⁶ The ETF suppresses Johnson and sensor 1/f noise current by the factor τ_0/τ .^{3,6} Note that in principle, the NEP implied by Johnson noise current fluctuations alone can be low in any sensor with high α and $P_b \gg GT/\alpha$ with or without ETF. In practice, however, stable low noise operation of a high α sensor with $P_b \gg GT/\alpha$ requires strong ETF. If the NEP is given only by thermal fluctuations, we can write

$$\text{NEP} = \sqrt{\gamma 4kT_0 (G/\bar{G}) (P + P_b) (1 + f)^2 / f} = \xi \sqrt{4kT_0 P}, \quad (5)$$

where $f = (T - T_0) / T_0$ is the fractional rise.

The bolometer used to test the VSB concept consists of a 40 nm thick film of W [$T_c \sim 95$ mK (Ref. 7)] etched to a 1.8×0.9 mm rectangle on a $300 \mu\text{m}$ thick silicon substrate. Electrical connections are made via Al wire bonds to lithographed Al contact pads covering the two 0.9 mm wide edges. The input coil of the dc-SQUID is in series with the sensor and the voltage bias is in parallel with the SQUID-sensor combination (see Fig. 2, inset). Constant voltage bias is obtained by current biasing a shunt resistor, whose $18 \text{ m}\Omega$ resistance is $\ll R$ ($\sim 160 \text{ m}\Omega$). The silicon substrate is attached directly to the $T_0 = 55$ mK mixing chamber of a dilution refrigerator. The weak thermal link G to the sensor is given by the poor coupling of electrons and phonons in the W film at this low temperature, which gives $n = 5$.⁸ All measurements were performed with the bolometer in the dark, which allows a precise knowledge of the power loading.

A measurement of the electrical responsivity of the bolometer is shown in Fig. 1. The sensor current I_s approaches a new equilibrium point after a step reduction in V_b . The ratio of the change in current to the change in power during this nonequilibrium period gives a responsivity of $S_I = -5.9 \times 10^5 \text{ A/W}$ for $V_b = 1.9 \times 10^{-6} \text{ V}$. This responsivity is 9% larger in magnitude than the predicted $1/V_b$. This discrepancy may be due to a damped overshoot from a resonance between the electrothermal feedback and the SQUID inductance,³ which can enhance the responsivity for $\omega \sim 1/\tau$. One way to avoid this resonance is to decrease the L/R time constant of the SQUID inductance and the sensor resistance. Alternatively, the bandwidth used can be restricted to $\omega < 1/\tau$, where this effect is not important. The measured

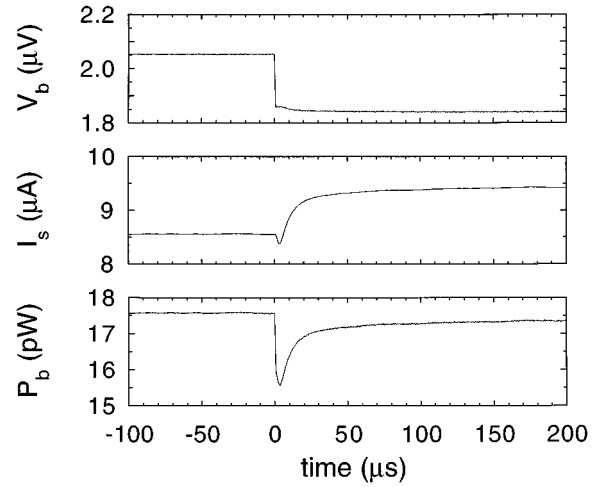


FIG. 1. Electrical responsivity measurement. Voltage step gives sensor power impulse, and the sensor reacts with a current response given by the responsivity. The thermal response time is $10 \mu\text{s}$. The responsivity is $5.9 \times 10^5 \text{ A/W}$ for $V_b = 1.85 \times 10^{-6} \text{ V}$.

time constant for $V_b = 1.9 \times 10^{-6} \text{ V}$ bias is equal to $10 \mu\text{s}$. The intrinsic time constant of this sensor is estimated to be ~ 1 ms from measurements of similar W films.⁴ The factor ~ 100 decrease in time constant is consistent with the factor ~ 80 predicted from Eq. (3) with $\alpha \sim 185$.

The measured NEP (shown in Fig. 2) is calculated by dividing the measured current noise referred to the SQUID input by the magnitude of the responsivity $1/V_b$. The series array of dc SQUIDs⁹ used for these experiments contributes significant noise ($i_n > 10 \text{ pA}/\sqrt{\text{Hz}}$) in the bandwidth of the plot. Since commercial single-SQUID ammeters have sufficiently low noise ($\sim 1 \text{ pA}/\sqrt{\text{Hz}}$ above 1 Hz) that they would not contribute significantly to the NEP of the detector, the NEP with the SQUID array noise subtracted in quadrature is also shown in Fig. 2. The minimum values of NEP with and without the SQUID noise are 3.3×10^{-17} and $2.5 \times 10^{-17} \text{ W}/\sqrt{\text{Hz}}$, respectively. Using Eq. (5), thermal fluctuation noise is expected to contribute $\sim 2 \times 10^{-17} \text{ W}/\sqrt{\text{Hz}}$ for $n = 5$. We calculate $G = 1.2 \times 10^{-9} \text{ W/K}$ from the measured \bar{G} , and we use $\gamma = 0.5$.¹⁰ The small discrepancy between the theoretical and measured NEPs is probably due, in

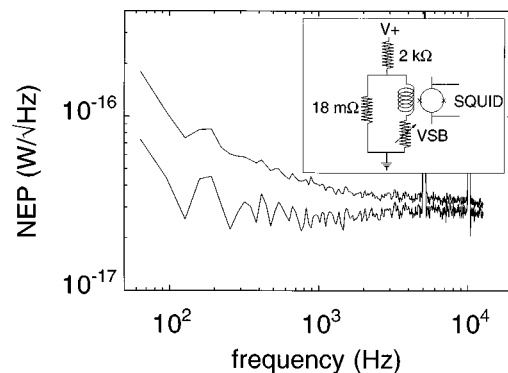


FIG. 2. NEP measurements. NEP (upper) and NEP with SQUID noise subtracted out in quadrature (lower). Minimum NEP with SQUID noise subtracted is $2.5 \times 10^{-17} \text{ W}/\sqrt{\text{Hz}}$ for a G of $1.2 \times 10^{-9} \text{ W/K}$ at 92 mK. (The inset shows the bolometer bias and readout circuit.)

part, to an underestimate of G . There is evidence that the silicon substrate heats to a temperature above that of the measured mixing chamber temperature. This heating would increase the estimated G , but the precise temperature is not known. Johnson noise is negligible because of the large α and strong ETF.^{3,6}

Bolometers are often operated at a frequency of a few Hz. To characterize the bolometer's performance in this frequency range, we used a square wave bias and demodulation at 2 kHz to circumvent the large low-frequency noise of the available SQUID. Despite problems as the bias passed through zero, we found an upper limit on the white noise of 6.2×10^{-17} W/ $\sqrt{\text{Hz}}$ with a noise corner at ~ 0.5 Hz. Better results could have been obtained with a single-SQUID ammeter.

When conventional semiconductor-thermistor bolometers are used at high frequencies, the value of G (and, hence, the thermal fluctuation noise) required for adequate speed can be larger than required by background loading even if C is rigorously minimized. In this regime, the useful figure of merit is $\text{NEP} \times \sqrt{\tau}$, which [from Eq. (3)] is proportional to $\alpha^{-1/2}$ for the VSB. In the measured bolometer this figure of merit is decreased by ETF by a factor of ~ 10 . Applications include rapid-scan Fourier transform spectroscopy, rapid scanning of an infrared telescope to avoid low-frequency atmospheric or system noise, and observation of rapidly varying infrared sources.

In applications where G is limited by the background power, the NEP can be expressed as $\xi \sqrt{4kT_0 P}$ as in Eq. (5) even if Johnson and amplifier noise terms are included.¹⁰ For astronomical applications, conventional semiconductor-thermistor bolometers are often operated with less than optimal temperature rise to avoid a large decrease in responsivity if P is underestimated at the time of fabrication. For this reason and because the Johnson noise term is comparable to the thermal fluctuation term, typical values for ξ are $\sim 5-6$.^{11,12} The G of the VSB must also be chosen from the largest estimated value of P . For a given G , the bias power is at its maximum value $P_{b-\text{max}}$ when the optical load is negligible. As P is increased, P_b decreases ($P + P_b$ is held constant in the extreme feedback limit) and the responsivity is constant. The sensor saturates when P approaches $P_{b-\text{max}}$. Simulations show that conservative operation ($P_{b-\text{max}} = 3 \times \text{estimated } P$) gives $\xi \sim 3$ for a weak link with $n = 2$. The NEP of the bolometer tested is close to the energy fluctuation limit and has a nearly optimal temperature rise with $f \sim 0.7$, but would have $\xi \sim 4.5$ for $P_{b-\text{max}} = 3 \times \text{estimated } P$ (SQUID noise subtracted). This ξ is high due to the high value of n for the thermal link that increases G/\bar{G} in Eq. (5). A comparison to the fast superconductor-insulator-normal junction bolometer is difficult since the published result⁸ ($\xi > 14$) is dominated by readout noise.

The thin film superconductive sensor is well adapted to either antenna coupling or absorber coupling to incident optical radiation. For frequencies above the energy gap, the sensor can serve as the resistive load for a lithographed antenna. Planar microwave filters and impedance transformers could be implemented. Alternately, a resistive absorber and the attached sensor could be isolated from the heat sink by any of the methods in use for composite bolometers.^{11,13,14}

Since the internal thermal time constant of the absorber-sensor combination is usually shorter than C/G , the speed increase due to ETF will be effective in reducing the time constant of this type of detector.

The VSB idea is directly applicable to high- T_c superconducting bolometers by using a high- T_c SQUID readout. Phase transitions such as those in the oxides of vanadium can produce large negative values of α at higher temperatures.¹⁵ For bolometers made with these materials, the benefits of strong ETF could be achieved with current bias and field-effect transistor voltage readout.

In summary, we have described a major improvement in bolometric detector technology. The time constant decrease due to ETF will allow bolometers to be used in new applications where conventional bolometers are too slow. In applications where the speed requirement limits G for a conventional bolometer, a substantial reduction in NEP should be possible. In applications where the background power limits G for a conventional bolometer, the VSB should yield essentially the ideal NEP with relaxed constraints on heat capacity. Both absorber- and antenna-coupled designs are realizable with lithographic techniques, facilitating implementation in arrays.

The authors thank James Bock, Sunil Golwala, Dan McCammon, and Shih-Fu Lee for helpful discussions. Viktor Hristov and Philip Mauskopf designed and built the ac-modulation apparatus. This work was supported in part by the Director, Office of Energy Research, Office of Basic Energy Sciences, Materials Sciences Division of the U.S. Department of Energy, under Contract No. DE-AC03-76SF00098 (PLR), by the National Science Foundation through the Center for Particle Astrophysics (Cooperative Agreement AST 91-20005) (ATL), DOE Grant No. DE-FG03-90ER50569 (SWN,BC), the Office of Naval Research under Grant Nos. N00014-92-J-1464 and N00014-92-F-003 (SWN,BC), and by NASA under Grant No. NAGW-4170 (KDI).

¹P. L. Richards, J. Appl. Phys. **76**, 1 (1994).

²J. Clarke, G. I. Hoffer, P. L. Richards, and N.-H. Yeh, J. Appl. Phys. **48**, 4865 (1977).

³K. D. Irwin, Appl. Phys. Lett. **66**, 1998 (1995).

⁴K. D. Irwin, S. W. Nam, B. Cabrera, B. Chugg, G. S. Park, R. P. Welty, and J. M. Martinis, IEEE Trans. Appl. Supercond. **5**, 2690 (1995).

⁵K. D. Irwin, Ph.D. thesis, Stanford University, p. 116 (1995).

⁶J. C. Mather, Appl. Opt. **21**, 1125 (1982).

⁷Thin tungsten film sputtered with voltage bias applied to substrate; see Ref. 4.

⁸M. Nahum and J. M. Martinis, Appl. Phys. Lett. **63**, 3075 (1993).

⁹R. P. Welty and J. M. Martinis, IEEE Trans. Magn. **MAG-27**, 2924 (1991).

¹⁰Sunil Golwala (personal communication) Also see related derivation in W. S. Boyle and K. F. Rogers, Jr., J. Opt. Soc. Am. **49**, 66 (1959).

¹¹D. C. Alsop, C. Inman, A. E. Lange, and T. Wilbanks, Appl. Opt. **31**, 6610 (1992).

¹²S. T. Tanaka, A. Clapp, M. Devlin, M. Fischer, C. Hagmann, A. E. Lange, and P. L. Richards, Proc. SPIE **1946**, 126 (1993).

¹³J. J. Bock, D. Chen, P. D. Mauskopf, and A. E. Lange, *Proceedings of the Future of IR and mm-wave Astronomy*, Saclay, France, 1994.

¹⁴P. M. Downey, A. D. Jeffries, S. S. Meyer, R. Weiss, F. J. Bachner, J. P. Donnelly, W. T. Lindley, R. W. Mountain, and D. J. S. Silversmith, Appl. Opt. **23**, 910 (1984).

¹⁵N. Tsuda, K. Nasu, A. Yanase, and K. Siratori, *Electronic Conduction in Oxides* (Springer-Verlag, Berlin, 1991).